TOPOLOGICAL MATTER

Evidence for Majorana bound states in an iron-based superconductor

Dongfei Wang[1,2]*, Lingyuan Kong[1,2]*, Peng Fan[1,2]*, Hui Chen[1], Shiyu Zhu[1,2], Wenyao Liu[1,2], Lu Cao[1,2], Yujie Sun[1,3], Shixuan Du[1,3,4], John Schneeloch[5], Ruidan Zhong[5], Genda Gu[5], Liang Fu[6], Hong Ding[1,2,3,4]†, Hong-Jun Gao[1,2,3,4]†

The search for Majorana bound states (MBSs) has been fueled by the prospect of using their non-Abelian statistics for robust quantum computation. Two-dimensional superconducting topological materials have been predicted to host MBSs as zero-energy modes in vortex cores. By using scanning tunneling spectroscopy on the superconducting Dirac surface state of the iron-based superconductor $FeTe_{0.55}Se_{0.45}$, we observed a sharp zero-bias peak inside a vortex core that does not split when moving away from the vortex center. The evolution of the peak under varying magnetic field, temperature, and tunneling barrier is consistent with the tunneling to a nearly pure MBS, separated from nontopological bound states. This observation offers a potential platform for realizing and manipulating MBSs at a relatively high temperature.

Majorana bound states (MBSs) in condensed-matter systems have attracted tremendous interest owing to their non-Abelian statistics and potential applications in topological quantum computation (*1*, *2*). A MBS is theoretically predicted to emerge as a spatially localized zero-energy mode in certain *p*-wave topological superconductors in one and two dimensions (*3*, *4*). Although the material realization of such *p*-wave superconductors has remained elusive, other platforms for MBSs have recently been proposed, using heterostructures between conventional *s*-wave superconductors and topological insulators (*5*), nanowires (*6*–*8*), quantum anomalous Hall insulators (*9*), or atomic chains (*10*), where the proximity effect on a spin-nondegenerate band creates a superconducting (SC) topological state. Various experimental signatures of MBSs (*11*–*14*) or Majorana chiral modes (*15*) have been observed in these heterostructures, but clear detection and manipulation of MBSs are often hindered by the contribution of nontopological bound states and complications of material interface.

Very recently, using high-resolution angle-resolved photoemission spectroscopy (ARPES), a potential platform for MBSs was discovered in the bulk superconductor $FeTe_{0.55}Se_{0.45}$, with a SC transition temperature T_c = 14.5 K and a simple crystal structure (Fig. 1A). Because of the topological band inversion between the p_z and d_{xz}/d_{yz} bands around the $\bar{\Gamma}$ point (*16*, *17*) and the multiband nature (Fig. 1B), this single material naturally has a spin-helical Dirac surface state, with an induced full SC gap and a small Fermi energy (Fig. 1C) (*18*); these properties would create favorable conditions for observing a pure MBS (*5*) that is isolated from other nontopological Caroli–de Gennes–Matricon bound states (CBSs) (*19*, *20*). The combination of high-T_c superconductivity and Dirac surface states in a single material removes the challenging interface problems in previous proposals and offers clear advantages for the detection and manipulation of MBSs.

Motivated by the above considerations, we carried out a high-resolution scanning tunneling microscopy/spectroscopy (STM/S) experiment on the surface of $FeTe_{0.55}Se_{0.45}$, which has a good atomic resolution that reveals the lattice formed by Te/Se atoms on the surface (Fig. 1D). We started with a relatively low magnetic field of 0.5 T along the *c* axis at a low temperature of 0.55 K, with a clear observation of vortex cores in Fig. 1E. At the vortex center, we observed a strong zero-bias peak (ZBP) with a full width at half maximum (FWHM) of 0.3 meV and an amplitude of 2 relative to the intensity just outside the gapped region. Outside of the vortex core, we clearly observed a SC spectrum with multiple gap features, similar to the ones observed in previous STM studies on the same material (*21*, *22*). These different SC gaps correspond well with the SC gaps on different Fermi surfaces of this material observed in previous ARPES studies (table S1) (*23*, *24*). A similar ZBP was reported previously (*22*).

We next demonstrate in Fig. 2 and fig. S4 (*24*) that across a large range of magnetic fields, the observed ZBP does not split when moving away from a vortex center. It can be clearly seen from Fig. 2, A to D, that the ZBP remains at the zero energy, while its intensity fades away when moving away from the vortex center. The nonsplit ZBP contrasts sharply with the split ZBP originating from CBS observed in conventional superconductors

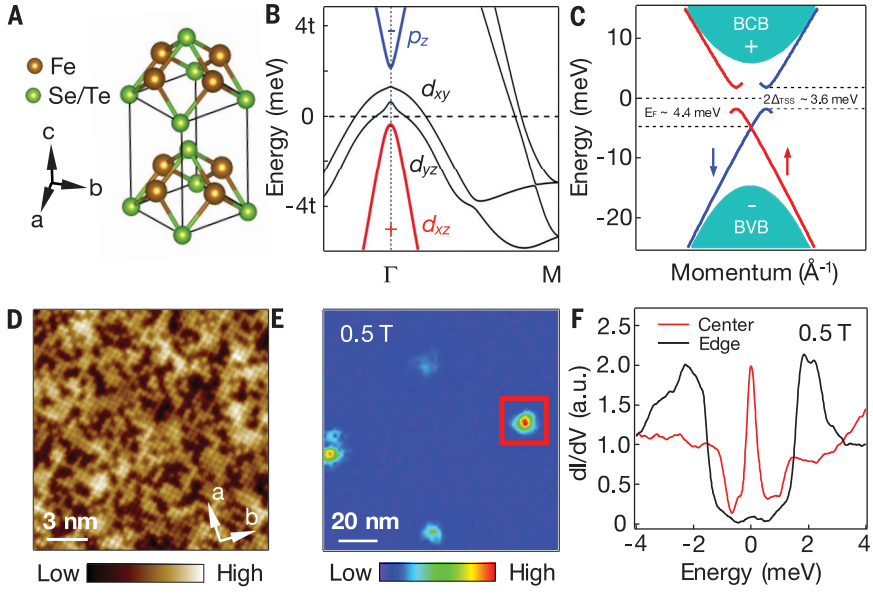

Fig. 1. Band structure and vortex cores of $FeTe_{0.55}Se_{0.45}$. (**A**) Crystal structure of $FeTe_{0.55}Se_{0.45}$. Axis a or b indicates one of the Fe–Fe bond directions. (**B**) A first-principle calculation of the band structure along the Γ-M direction. In the calculations, t = 100 meV, whereas t ~ 12 to 25 meV from ARPES experiments, largely depending on the bands (*23*). [Adapted from (*18*), figure 1C] (**C**) Summary of SC topological surface states on this material observed by ARPES from (*18*). (**D**) STM topography of $FeTe_{0.55}Se_{0.45}$ (scanning area, 17 nm by 17 nm). (**E**) Normalized zero-bias conductance (ZBC) map measured at a magnetic field of 0.5 T, with the area 120 nm by 120 nm. (**F**) A sharp ZBP in a *dI*/*dV* spectrum measured at the vortex core center indicated in the red box in (E). Settings are sample bias, V_s = −5 mV; tunneling current, I_t = 200 pA; and temperature, T = 0.55 K.

[1]Beijing National Laboratory for Condensed Matter Physics and Institute of Physics, Chinese Academy of Sciences (CAS), Beijing 100190, China. [2]School of Physical Sciences, University of Chinese Academy of Sciences, Beijing 100190, China. [3]CAS Center for Excellence in Topological Quantum Computation, University of Chinese Academy of Sciences, Beijing 100190, China. [4]Collaborative Innovation Center of Quantum Matter, Beijing 100190, China. [5]Condensed Matter Physics and Materials Science Department, Brookhaven National Laboratory, Upton, NY 11973, USA. [6]Department of Physics, Massachusetts Institute of Technology, Cambridge, MA 02139, USA.
*These authors contributed equally to this work.
†Corresponding author. Email: dingh@iphy.ac.cn (H.D.); hjgao@iphy.ac.cn (H.-J.G.)

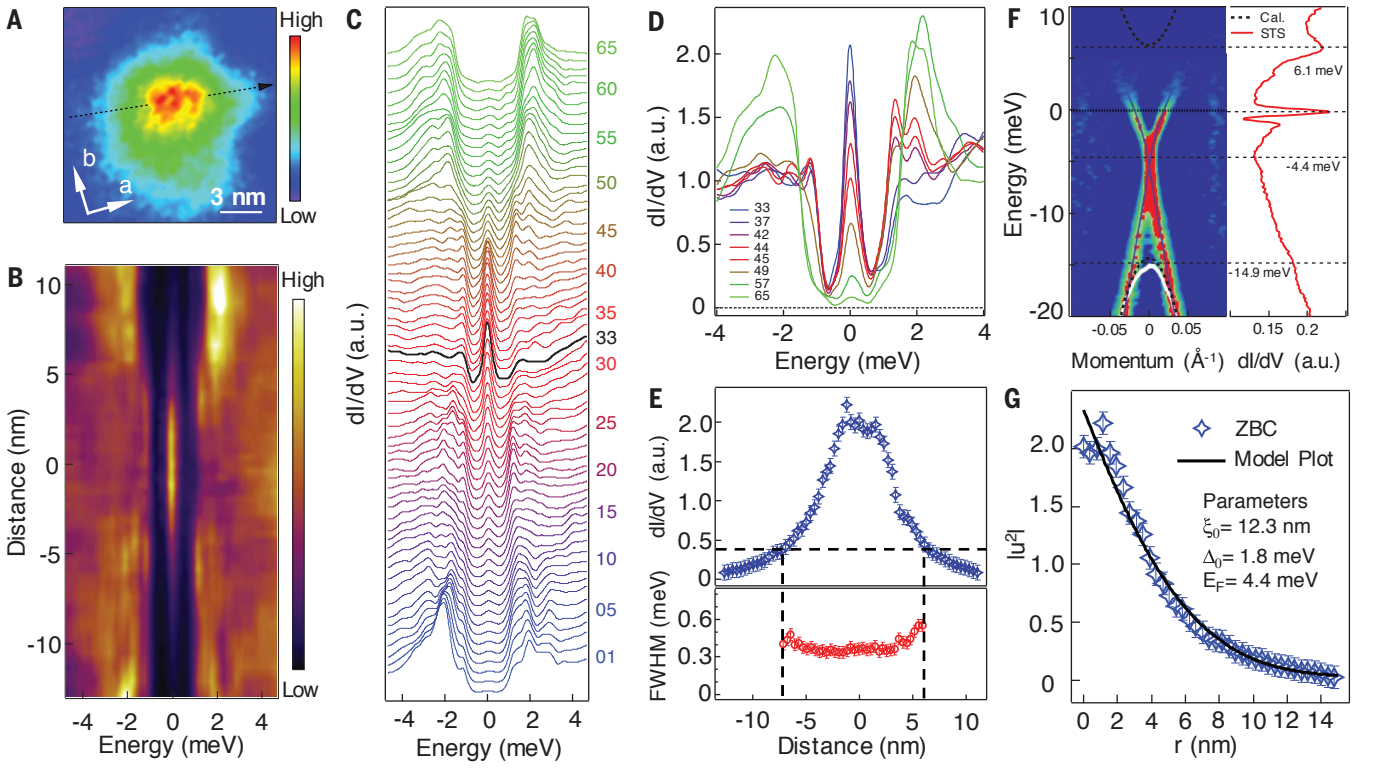

Fig. 2. Energetic and spatial profile of ZBPs. (**A**) A ZBC map (area, 15 nm by 15 nm) around vortex cores. (**B**) A line-cut intensity plot along the black dashed line indicated in (A). (**C**) A waterfall-like plot of (B) with 65 spectra, with the black curve corresponding to the one in the core center. (**D**) An overlapping display of eight *dI/dV* spectra selected from (C). (**E**) Spatial dependence of the height (top) and FWHM (bottom) of the ZBP. (**F**) Comparison between ARPES and STS results. (Left) ARPES results on the topological surface states. [Adapted from (*18*)] Black dashed curves are extracted from a first-principle calculation (*37*), with the calculated data rescaled to match the energy positions of the Dirac point and the top of the bulk valence band (BVB). (Right) A *dI/dV* spectrum measured from −20 to 10 meV. (**G**) Comparison between the measured ZBP peak intensity with a theoretical calculation of MBS spatial profile [(*24*), part VIII]. The data in (B) to (G) are normalized by the integrated area of each *dI/dV* spectrum. Settings are V_s = −5 mV, I_t = 200 pA, T = 0.55 K, and perpendicular magnetic field ($B_\perp$) = 0.5 T.

(*19*, *20*) and is consistent with tunneling into an isolated MBS in a vortex core of a SC topological material (*5*, *25*–*27*). We then extracted the position-dependent values of the ZBP height and width using simple Gaussian fits of the data in Fig. 2C and obtained the spatial profile shown in Fig. 2E; the decaying profile has a nearly constant line width of ~0.3 meV in the center, which is close to the total width (~0.28 meV) contributed from the STM energy resolution [~0.23 meV as shown in part I of (*24*)] and the thermal broadening [$3.5k_BT$ at 0.55 K ~ 0.17 meV, where k_B is the Boltzmann constant]. We further compared the observed ZBP height with a theoretical MBS spatial profile obtained by solving the Bogoliubov–de Gennes equation analytically (*5*, *25*) or numerically (*26*, *27*). By using the parameters of E_F = 4.4 meV, Δ_{sc} = 1.8 meV, and $\xi_0 = v_F/\Delta_{sc}$ = 12 nm, which are obtained directly from the topological surface state by our scanning tunneling spectroscopy (STS) and ARPES results (Fig. 2F) (*18*), the theoretical MBS profile matches well the experimental one (Fig. 2G).

The observation of a nonsplit ZBP, which is different from the split ZBP observed in a vortex of the $Bi_2Te_3/NbSe_2$ heterostructure (*13*, *28*, *29*), indicates that the MBS peak in our system is much less contaminated by nontopological CBS peaks, which is made possible by the large Δ_{sc}/E_F ratio in this system. In a usual topological insulator/superconductor heterostructure, this ratio is tiny, on the order of 10^{-3} to 10^{-2} (*28*). This has been shown to induce, in addition to the MBS at the zero energy, many CBSs, whose level spacing is proportional to Δ_{sc}^2/E_F. As a result, these CBSs were crowded together very close to the zero energy, making difficult a clean detection of MBS from the *dI/dV* spectra (*29*). However, on the surface of $FeTe_{0.55}Se_{0.45}$, the value of Δ_{sc}^2/E_F is ~0.74 meV, which is sufficiently large to push most CBSs away from the zero energy (*24*), leaving the MBS largely isolated and unspoiled. A large energy separation (0.7 meV) between the ZBP and the CBS was observed in fig. S3, E to H, which is in agreement with Δ_{sc}^2/E_F of the topological surface states [(*24*), part IV]. Also, all the bulk bands in this multiband material have fairly small values of E_F owing to large correlation-induced mass renormalization, ranging from a few to a few tens of millielectron volts; thus, their values of Δ_{sc}^2/E_F are also quite large (>0.2 meV) (table S1) (*24*). These large bulk ratios enlarge the energy-level spacing of CBSs inside the bulk vortex line, which helps reduce quasiparticle poisoning of the MBS at low temperature [(*24*), part II].

It has been predicted (*30*) that the width of the ZBP from tunneling into a single isolated MBS is determined by thermal smearing ($3.5k_BT$), tunneling broadening, and STM instrumentation resolution. We measured the tunneling barrier evolution of the ZBP (Fig. 3A). Robust ZBPs can be observed over two orders of magnitude in tunneling barrier conductance, with the width barely changing (Fig. 3B). Also, the line width of ZBPs is almost completely limited by the combined broadening of energy resolution and STM thermal effect, suggesting that the intrinsic width of the MBS is much smaller, and our measurements are within the weak tunneling regime.

However, we did observe some other ZBPs with a larger broadening (Fig. 3C). A larger ZBP broadening is usually accompanied with a softer SC gap, or the FWHM of ZBP increases with increasing subgap background conductance. The subgap background conductance, which is determined by factors such as the strength of scattering from disorder and quasiparticle interactions (*31*–*33*), introduces a gapless fermion bath that can poison the MBS, as explained previously (*34*). The effect of quasiparticle poisoning is to reduce the MBS amplitude and increase its width. This scenario is likely the origin of a

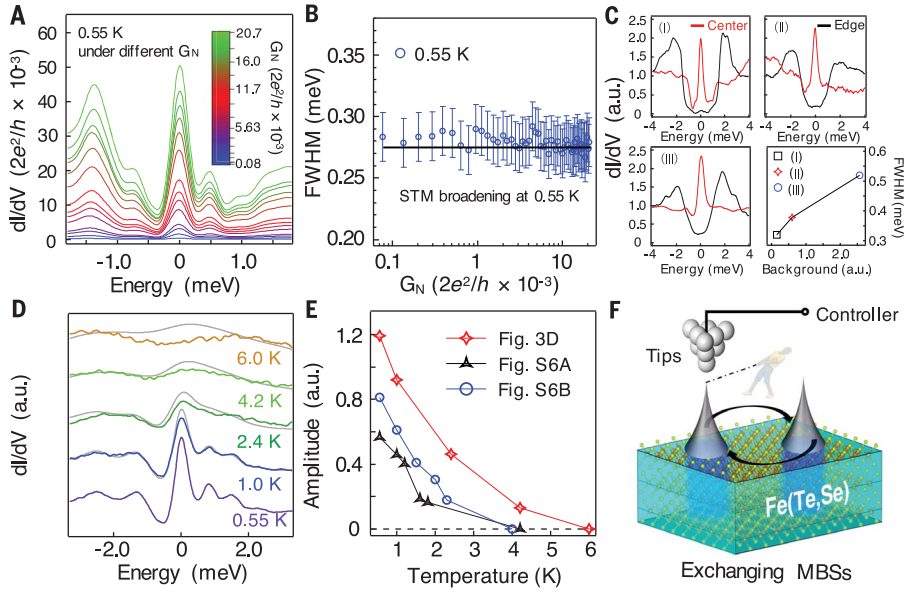

Fig. 3. Temperature and tunneling barrier evolution of ZBPs. (**A**) Evolution of ZBPs, with tunneling barrier measured at 0.55 K. $G_N \equiv I_t/V_s$, which corresponds to the energy-averaged conductance of normal states and represents the conductance of the tunneling barrier. I_t and V_s are the STS setpoint parameters. (**B**) FWHM of ZBPs at 0.55 K under different tunneling barriers. The black solid line is the combined effect of energy resolution (0.23 meV) (*24*) and tip thermal broadening ($3.5k_BT$) at 0.55 K. (**C**) FWHM of ZBP at the center of the vortex core is larger when the SC gap around the vortex core is softer. Background is defined as an integrated area from –1 to +1 meV of the spectra at the core edge. (**D**) Temperature evolution of ZBPs in a vortex core. The gray curves are numerically broadened 0.55 K data at each temperature. (**E**) Amplitude of the ZBPs shown in (D) and fig. S6 (*24*) under different temperatures. The amplitude is defined as the peak-valley difference of the ZBP. (**F**) Schematic of a possible way for realizing non-Abelian statistics in an ultralow-temperature STM experiment that may have an ability to exchange MBSs on the surface of Fe(Te, Se). (A) and (B) show the absolute value of conductance; $B_\perp$ = 2.5 T. In (D) and (E), the data are normalized by integrated area; V_s = –10 mV, I_t = 100 pA, T = 0.55 K, and $B_\perp$ = 4 T.

larger broadening of ZBP accompanied by a softer gap.

It has been pointed out by previous theoretical studies (*35*–*37*) that the condition of a bulk vortex line, such as its chemical potential, has substantial influences on the Majorana mode on the surface by the vortex phase transition. In order to further characterize the effects of bulk vortex lines, we have monitored the temperature evolution of a ZBP. As shown in Fig. 3D, the ZBP intensity measured at a vortex center decreases with increasing temperature and becomes extremely weak at 4.2 K and totally invisible at 6.0 K. A peak associated with a CBS would persist to higher temperatures and exhibit simple Fermi-Dirac broadening up to about $T_c/2$ (~8 K), below which the SC gap amplitude is almost constant, as observed in our previous ARPES measurement (*18*). Our observation (Fig. 3D) contradicts this expectation and indicates an additional suppression mechanism that is likely related to the poisoning of MBS by thermally excited quasiparticles. From the extraction of ZBP amplitude measured on several different vortices (three cases are shown in Fig. 3E), we found that most of the observed ZBPs vanish around 3 K, which is higher than the temperature in many previous Majorana platforms (*11*, *38*). This vanishing temperature is comparable with the energy level spacing of the bulk vortex line as discussed above; thus, the temperature dependence we found is consistent with a case of a MBS poisoned by thermally induced quasiparticles inside the bulk vortex line (*24*).

Our observations provide strong evidence for tunneling to an isolated MBS; many alternative trivial explanations [(*24*), part III] cannot account for all the observed features. It is technically possible to move a vortex by a STM tip, which in principle can be used to exchange MBSs inside vortices (Fig. 3F), consequently demonstrating non-Abelian statistics under a sufficiently low ($k_BT \ll \Delta_{sc}^2/E_F$) temperature (*2*). The high transition temperature and large SC gaps in this superconductor offer a promising platform to fabricate robust devices for topological quantum computation.

REFERENCES AND NOTES

1. A. Y. Kitaev, *Ann. Phys.* **303**, 2–30 (2003).
2. C. Nayak, S. H. Simon, A. Stern, M. Freedman, S. Das Sarma, *Rev. Mod. Phys.* **80**, 1083–1159 (2008).
3. A. Y. Kitaev, *Phys. Uspekhi* **44** (10S), 131–136 (2001).
4. N. Read, D. Green, *Phys. Rev. B* **61**, 10267–10297 (2000).
5. L. Fu, C. L. Kane, *Phys. Rev. Lett.* **100**, 096407 (2008).
6. R. M. Lutchyn, J. D. Sau, S. Das Sarma, *Phys. Rev. Lett.* **105**, 077001 (2010).
7. Y. Oreg, G. Refael, F. von Oppen, *Phys. Rev. Lett.* **105**, 177002 (2010).
8. A. C. Potter, P. A. Lee, *Phys. Rev. Lett.* **105**, 227003 (2010).
9. X.-L. Qi, T. L. Hughes, S.-C. Zhang, *Phys. Rev. B* **82**, 184516 (2010).
10. S. Nadj-Perge, I. K. Drozdov, B. A. Bernevig, A. Yazdani, *Phys. Rev. B* **88**, 020407 (2013).
11. V. Mourik *et al.*, *Science* **336**, 1003–1007 (2012).
12. S. Nadj-Perge *et al.*, *Science* **346**, 602–607 (2014).
13. H.-H. Sun *et al.*, *Phys. Rev. Lett.* **116**, 257003 (2016).
14. M. T. Deng *et al.*, *Science* **354**, 1557–1562 (2016).
15. Q.-L. He *et al.*, *Science* **357**, 294–299 (2017).
16. Z.-J. Wang *et al.*, *Phys. Rev. B* **92**, 115119 (2015).
17. X.-X. Wu, S. Qin, Y. Liang, H. Fan, J. Hu, *Phys. Rev. B* **93**, 115129 (2016).
18. P. Zhang *et al.*, *Science* **360**, 182–186 (2018).
19. C. Caroli, P. G. de Gennes, J. Matricon, *Phys. Lett.* **9**, 307–309 (1964).
20. H. F. Hess, R. B. Robinson, J. V. Waszczak, *Phys. Rev. Lett.* **64**, 2711–2714 (1990).
21. T. Hanaguri, S. Niitaka, K. Kuroki, H. Takagi, *Science* **328**, 474–476 (2010).
22. F. Massee *et al.*, *Sci. Adv.* **1**, e1500033 (2015).
23. H. Miao *et al.*, *Phys. Rev. B* **85**, 094506 (2012).
24. Materials and methods are available as supplementary materials.
25. Y. Wang, L. Fu, *Phys. Rev. Lett.* **119**, 187003 (2017).
26. C.-K. Chiu, M. J. Gilbert, T. L. Hughes, *Phys. Rev. B* **84**, 144507 (2011).
27. L.-H. Hu, C. Li, D.-H. Xu, Y. Zhou, F.-C. Zhang, *Phys. Rev. B* **94**, 224501 (2016).
28. J.-P. Xu *et al.*, *Phys. Rev. Lett.* **112**, 217001 (2014).
29. J.-P. Xu *et al.*, *Phys. Rev. Lett.* **114**, 017001 (2015).
30. F. Setiawan, C.-X. Liu, J. D. Sau, S. Das Sarma, *Phys. Rev. B* **96**, 184520 (2017).
31. S. Das Sarma, A. Nag, J. D. Sau, *Phys. Rev. B* **94**, 035143 (2016).
32. Y. Yin *et al.*, *Phys. Rev. Lett.* **102**, 097002 (2009).
33. C. Renner, A. D. Kent, P. Niedermann, O. Fischer, F. Lévy, *Phys. Rev. Lett.* **67**, 1650–1652 (1991).
34. J. R. Colbert, P. A. Lee, *Phys. Rev. B* **89**, 140505 (2014).
35. P. Hosur, P. Ghaemi, R. S. K. Mong, A. Vishwanath, *Phys. Rev. Lett.* **107**, 097001 (2011).
36. H.-H. Hung, P. Ghaemi, T. L. Hughes, M. J. Gilbert, *Phys. Rev. B* **87**, 035401 (2013).
37. G. Xu, B. Lian, P. Tang, X.-L. Qi, S.-C. Zhang, *Phys. Rev. Lett.* **117**, 047001 (2016).
38. F. Nichele *et al.*, *Phys. Rev. Lett.* **119**, 136803 (2017).

ACKNOWLEDGMENTS

We thank Q. Huan, H. Isobe, X. Lin, X. Wu, and K. Yang for technical assistance and P. A. Lee, T. K. Ng, S. H. Pan, G. Xu, J.-X. Yin, F. C. Zhang, and P. Zhang for useful discussions. **Funding:** This work at IOP is supported by grants from the Ministry of Science and Technology of China (2013CBA01600, 2015CB921000, 2015CB921300, and 2016YFA0202300), the National Natural Science Foundation of China (11234014, 11574371, and 61390501), and the Chinese Academy of Sciences (XDPB08-1, XDB07000000, and XDPB0601). L.F. and G.G. are supported by the U.S. Department of Energy (DOE) (DE-SC0010526 and DE-SC0012704, respectively). J.S. and R.Z. are supported by the Center for Emergent Superconductivity, an Energy Frontier Research Center funded by the U.S. DOE. **Author contributions:** H.D., H.-J.G., L.K., Y.S., and S.D. designed the experiments. D.W., L.K., P.F., H.C., S.Z., W.L., and L.C. performed the STM experiments. J.S., R.Z., and G.G. provided the samples. L.F. provided theoretical models and explanations. All the authors participated in analyzing the experimental data, plotting the figures, and writing the manuscript. H.D. and H.-J.G. supervised the project. **Competing interests:** The authors declare that they have no competing interests. **Data and materials availability:** The data presented in this paper can be found in the supplementary materials.

SUPPLEMENTARY MATERIALS

www.sciencemag.org/content/362/6412/333/suppl/DC1
Materials and Methods
Supplementary Text
Figs. S1 to S7
Table S1
References (*39*–*69*)
Data File S1

22 June 2017; resubmitted 11 December 2017
Accepted 27 July 2018
Published online 16 August 2018
10.1126/science.aao1797

Science

Evidence for Majorana bound states in an iron-based superconductor

Dongfei Wang, Lingyuan Kong, Peng Fan, Hui Chen, Shiyu Zhu, Wenyao Liu, Lu Cao, Yujie Sun, Shixuan Du, John Schneeloch, Ruidan Zhong, Genda Gu, Liang Fu, Hong Ding and Hong-Jun Gao

Science **362** (6412), 333-335.
DOI: 10.1126/science.aao1797originally published online August 16, 2018

An iron home for Majoranas

The surface of the iron-based superconductor $FeTe_{0.55}Se_{0.45}$ has been identified as a potential topological superconductor and is expected to host exotic quasiparticles called the Majorana bound states (MBSs). Wang *et al.* looked for signatures of MBSs in this material by using scanning tunneling spectroscopy on the vortex cores formed by the application of a magnetic field. In addition to conventional states, they observed the characteristic zero-bias peaks associated with MBSs and were able to distinguish between the two, owing to the favorable ratios of energy scales in the system.

Science, this issue p. 333